

Investigation of Equivalent System Modeling and Dynamic Characteristics Using Reduced Models

Young-Sug Shin* and In Lee†

Korea Advanced Institute of Science and Technology, Taejeon 305-701, Republic of Korea

An improved approach of updating the initial finite element models in comparison with a modal test is presented. This is accomplished by using the reduced models dynamically equivalent to the initial models. The degrees of freedom (DOF) in the reduced models include the generalized coordinates besides the measurement points for a modal test. Therefore, these reduced models can take into account the inertia force at unmeasured DOF and preserve the dynamic characteristics of the initial analytical models regardless of the measurement points. These reduced models are used for a direct analysis/experiment correlation with modal test data. Numerical simulation results are presented to show the effectiveness of these reduced models in the parametric correction of the analytical finite element models.

Nomenclature

$[\tilde{K}]$	= Guyan-reduced stiffness matrix
$[K_a]$	= nominal stiffness matrix of the initial finite element model
$[K_b]$	= stiffness matrix for exactly modeled parts in the initial finite element model
$[K_j]$	= j th submatrix for the assumed stiffness in the initial finite element model
$[\hat{K}_k]$	= stiffness matrix of the test models of k degrees of freedom (DOF)
$[\tilde{K}_k]$	= stiffness matrix of the present TAM of k DOF
$[K_n]$	= stiffness matrix of the initial finite element models of n DOF
$[\hat{K}_n]$	= stiffness matrix of the Craig-Bampton finite element models of n DOF
$[\tilde{M}]$	= Guyan-reduced mass matrix
$[\hat{M}_k]$	= mass matrix of the test models of k DOF
$[\tilde{M}_k]$	= mass matrix of the present test-analysis model (TAM) of k DOF
$[M_n]$	= mass matrix of the initial finite element models of n DOF
$[\hat{M}_n]$	= mass matrix of the Craig-Bampton finite element models of n DOF
p	= total number of submatrices
$[Q]$	= orthonormal matrix in a singular value decomposition
$\{q_n\}$	= physical displacement vectors
s_j	= j th scaling factor
$[T_{CB}]$	= Craig-Bampton transformation matrix
$[T_{mix}]$	= transformation matrix to make the present TAM
$[T_{SEREP}]$	= SEREP transformation matrix
$[T_{\tilde{z}}]$	= modal matrix obtained from the unmeasured DOF of the Craig-Bampton finite element models
$[U]$	= modal matrix obtained from the unmeasured DOF of the test models
$[\Delta\Omega]$	= inertia force effect matrix
ξ	= generalized coordinates in the Craig-Bampton component synthesis method
$[\Sigma]$	= singular value matrix in a singular value decomposition
$[\Phi]$	= modal matrix obtained from the Craig-Bampton finite element models
$\{\phi\}$	= individual eigenvectors obtained from the Craig-Bampton finite element models

$[\Psi]$	= modal matrix obtained from test models
$\{\psi\}$	= individual eigenvectors obtained from test models
$[\Omega]$	= diagonal eigenvalue matrix

Introduction

IN the case of the lightweight spacecraft's structural design, an accurate system model is essential for the flutter suppression, stress analysis, and design of control/structure interactions. To model a structural dynamic system accurately, the stiffness of connected parts in the structure should be exactly identified. When a structural dynamic system is modeled with a finite element method, the stiffness of connected parts is usually modeled with the assumption of rigid connection between components. However, such modeling cannot represent exactly the stiffness of connected parts. Therefore, the correction of the assumed stiffness at connected parts in the finite element model should be performed through test-analysis correlation in the modal test. For the initial finite element models' correction to take place, two kinds of model are used because the structure system modeled by the finite element method has far more degrees of freedom (DOF) than the modal survey test. One model is the finite element model itself, and the other is a reduced model. When the finite element model is used, a structural connectivity is preserved,¹ but the matrix size becomes very large in solving an eigenproblem for the large-scale structure. When the reduced model^{2,3} is used, the model is used for a direct test-analysis correlation. However, the accuracy^{4,5} depends on the reduction schemes. Therefore, an exactly reduced representation of the initial finite element model is essential to obtain efficiently an improved model of structural dynamic system.

For a direct test-analysis correlation the finite element models should be reduced to match the results of a modal test. This reduced model is called the test-analysis model (TAM). The previously reported TAM includes only the measured DOF.²⁻⁸ Such TAM are based on the Guyan reduction method. However, the Guyan TAM cannot preserve exactly the measured modal dynamic characteristics according to the number and locations of measurement. This inaccuracy arises from the fact that the Guyan TAM cannot properly take into account the inertia force effect at unmeasured DOF. That is to say, the Guyan TAM condenses the identified dynamics obtained from a test into a smaller dimensional space of a reduced model. Many efforts to overcome drawbacks of Guyan TAM have been focused on the reflecting inertia force effect,^{3,6,7} but they are still approximate. Recently, Denoyer and Peterson⁸ minimized the error between the measured and analytical static flexibility matrices using a gradient search method. However, Denoyer uses basically the Guyan reduction method to formulate the flexibility matrices having only measurement DOF.

In this paper, other than the previously reported TAM, the generalized coordinates are used in addition to the measurement points

Received 16 November 1998; revision received 22 May 1999; accepted for publication 24 May 1999. Copyright © 1999 by the American Institute of Aeronautics and Astronautics, Inc. All rights reserved.

*Graduate Research Assistant, Department of Aerospace Engineering.

†Professor, Department of Aerospace Engineering; inlee@asdl.kaist.ac.kr. Senior Member AIAA.

to make the present TAM when the number of identified modes of a modal test are more than that of accelerometers.⁹ The generalized coordinates are like the Craig–Bampton component mode synthesis method¹⁰ and determined from the generalized inverse problem of modal test results. To make a present TAM, the finite element models are partitioned into a set of measurement points and a set of generalized coordinates using a Craig–Bampton transformation matrix. Then, the Craig–Bampton finite element models are reduced to match the test models. Here, the test models consist of the generalized coordinate DOF and the measured DOF. The generalized coordinates of the test model are determined using a method of singular-value decomposition in the inverse vibration problem, which is composed of the experimentally identified modes of a modal test. These test models preserve the full eigenspectrum measured from a test and are called the minimal-order resultant mass and stiffness matrices.⁹ To reduce the Craig–Bampton finite element models, the System Equivalent Reduction Expansion Process (SEREP) defined as the exact modal reduction method¹¹ is used. The modal matrix used for the SEREP method is obtained from the eigensolutions of the Craig–Bampton finite element models. Until now, the eigenvectors used in the inverse matrix of the SEREP method have been chosen from only measured DOF of the eigensolutions of the general finite element models. However, in this paper the eigenvectors are chosen additionally from the generalized coordinates of the eigensolution of the Craig–Bampton finite element models. Therefore, the present TAM can be the reduced representation exactly equivalent to the Craig–Bampton finite element models and can be matched with the test models having the generalized coordinate DOF.

For a direct correction of the initial model's stiffness using the present TAM, stiffness submatrices with scaling factors, which represent a perturbation from the exact, are used.⁴ Stiffness submatrices are made by grouping elements of the same stiffness characteristics, which can be used for the unknown stiffness of connected parts. Unknown scaling factors are solved by using a least-square method. Therefore, the parametric correction of the initial finite element model can be performed with scaling factors. Numerical simulation results are presented to demonstrate the effectiveness of the present TAM for the Kabe's model¹ with eight DOF and the cantilever beam structure.

Formulation

Craig–Bampton Matrices Formulation

The equation of motion of undamped n -DOF linear system modeled with the finite element method is represented by

$$[M_n]\{\ddot{q}_n\} + [K_n]\{q_n\} = \{0\} \quad (1)$$

where $[M_n]$ and $[K_n]$ are the system mass and stiffness matrices, respectively, and $\{q_n\}$ is a vector containing physical displacements. Equation (1) having n DOF is partitioned into a set of measured DOF $\{q_m\}$ and unmeasured DOF $\{q_i\}$ as follows:

$$\begin{bmatrix} M_{mm} & M_{mi} \\ M_{im} & M_{ii} \end{bmatrix} \begin{Bmatrix} \ddot{q}_m(t) \\ \ddot{q}_i(t) \end{Bmatrix} + \begin{bmatrix} K_{mm} & K_{mi} \\ K_{im} & K_{ii} \end{bmatrix} \begin{Bmatrix} q_m(t) \\ q_i(t) \end{Bmatrix} = \{0\} \quad (2)$$

In the Craig–Bampton component mode synthesis method,¹⁰ displacements at unmeasured DOF are expressed as

$$q_i = -K_{ii}^{-1}K_{mi}^T q_m + T_\xi \xi \quad (3)$$

where ξ are the generalized coordinates for unmeasured DOF and T_ξ is the modal matrix composed of the mass normalized eigenvectors satisfying the eigenproblem equations (4) and (5):

$$K_{ii} T_\xi = M_{ii} T_\xi \Omega_\xi^2 \quad (4)$$

$$T_\xi^T K_{ii} T_\xi = \Omega_\xi^2, \quad T_\xi^T M_{ii} T_\xi = I \quad (5)$$

Using Eq. (3), the Craig–Bampton transformation matrix is defined as

$$[T_{CB}] = \begin{bmatrix} I & 0 \\ -K_{ii}^{-1}K_{mi}^T & T_\xi \end{bmatrix} \quad (6)$$

Using Eq. (6), the Craig–Bampton finite element models of Eq. (2) are given by

$$[\hat{K}_n] = [T_{CB}]^T [K_n] [T_{CB}] \quad (7)$$

$$[\hat{M}_n] = [T_{CB}]^T [M_n] [T_{CB}] \quad (8)$$

Formulation of the Test Model (Minimal-Order Resultant Mass and Stiffness Matrices)

Meanwhile, the test model, which is used as the result of the modal test in the direct test/analysis correlation, can be generated from the modal test results to include the generalized coordinate DOF. If this test model can predict all measured modal characteristics, such a model is the minimal-order resultant mass and stiffness matrices.⁹ In Ref. 9 the method of minimal-order resultant mass and stiffness matrices was developed very well, and we will follow their review. When the experimentally identified modes of a modal test are more than accelerometers, the inverse vibration problem of the minimal-order system matrices can be formulated to make the test models. If the $m \times k$ modal matrix Ψ_m is obtained from a modal test, the $k \times k$ modal matrix Ψ_k is assumed as

$$[\Psi_k] = [\psi_1, \psi_2, \dots, \psi_k] = \begin{bmatrix} \Psi_m \\ \Psi_g \end{bmatrix} \quad (9)$$

where ψ_i , $i = 1, 2, \dots, k$ represent the individual eigenvectors and k , m , and g denote the number of measured modes, accelerometers, and generalized coordinates, respectively. And Ψ_g denotes the $(k - m) \times k$ modal submatrix corresponding to the generalized coordinates, which will be solved in the inverse vibration problem of Eq. (10). When the rigid body motion does not exist, the inverse vibration problem for the modal matrices of Eq. (9) can be defined as

$$[\hat{K}_k]^{-1} = [\Psi_k][\Omega_k]^{-1}[\Psi_k]^T, \quad [\hat{M}_k]^{-1} = [\Psi_k][\Psi_k]^T \quad (10)$$

where $[\Omega_k]$ is the diagonal matrix of k measured eigenvalues. The eigenproblem for the matrices of Eq. (10) is partitioned into a measured set m and a generalized coordinate set g as follows:

$$\begin{bmatrix} \bar{K} & 0 \\ 0 & \Omega_g \end{bmatrix} \begin{bmatrix} \Psi_m \\ \Psi_g \end{bmatrix} = \begin{bmatrix} \bar{M} & M_c \\ M_c^T & I \end{bmatrix} \begin{bmatrix} \Psi_m \\ \Psi_g \end{bmatrix} [\Omega_k] \quad (11)$$

where Ψ_m and Ψ_g are mass normalized eigenvectors such that

$$\begin{bmatrix} \Psi_m^T & \Psi_g^T \end{bmatrix} \begin{bmatrix} \bar{K} & 0 \\ 0 & \Omega_g \end{bmatrix} \begin{bmatrix} \Psi_m \\ \Psi_g \end{bmatrix} = [\Omega_k] \quad (12)$$

and $[\bar{K}]$, $[\bar{M}]$ are the Guyan-reduced mass and stiffness matrices, respectively:

$$[\bar{K}] = [\Psi_m][\Omega_k][\Psi_m]^T \quad (13)$$

$$[\bar{M}] = [\bar{K}][\Psi_m][\Omega_k][\Psi_m]^T [\bar{K}] \quad (14)$$

Although Ψ_g and Ω_g are unknown in Eq. (11), the inertia force effect matrix can be calculated as

$$\Psi_g^T \Omega_g \Psi_g = \Omega_k - \Psi_m^T (\Psi_m \Omega_k^{-1} \Psi_m^T)^{-1} \Psi_m = \Delta \Omega \quad (15)$$

that is, the inertia force effect matrix $\Delta \Omega$ is determined from the difference between the measured eigenvalues Ω_k and the projection of the reduced stiffness through the measured mode shapes Ψ_m . The rank of Ω_k is k , whereas the rank of $\Psi_m^T \bar{K} \Psi_m$ is m . Therefore, the $(k - m)$ nonzero singular values can be determined using a singular-value decomposition for $\Delta \Omega$ as

$$\text{SVD}(\Delta \Omega) = Q \Sigma Q^T = Q_g \Sigma_g Q_g^T \quad (16)$$

where Q_g is a basis for the g -augmented generalized coordinates and composed of the orthonormal vectors of the singular values. The

inverse vibration problem, which is augmented with Q_g obtained from Eq. (16), can be defined as

$$\begin{bmatrix} \bar{K} & 0 \\ 0 & K_g \end{bmatrix} = \begin{bmatrix} \Psi_m \\ Q_g^T \end{bmatrix}^{-T} [\Omega_k] \begin{bmatrix} \Psi_m \\ Q_g \end{bmatrix}^{-1}$$

$$\begin{bmatrix} \bar{M} & \bar{M}_c \\ \bar{M}_c^T & M_g \end{bmatrix} = \begin{bmatrix} \Psi_m \\ Q_g^T \end{bmatrix} [\Psi_m^T \quad Q_g]^{-1} \quad (17)$$

For consistency with the definition of ξ in Eq. (3), eigenvectors at augmented generalized coordinates of g are mass normalized as

$$K_g U = M_g U \Omega_g, \quad U^T K_g U = \Omega_g, \quad U^T M_g U = I \quad (18)$$

The test models are obtained as the minimal-order resultant mass and stiffness matrices of Eq. (10) after the following transformation:

$$[\hat{K}_k] = \begin{bmatrix} I & 0 \\ 0 & U^T \end{bmatrix} \begin{bmatrix} \bar{K} & 0 \\ 0 & K_g \end{bmatrix} \begin{bmatrix} I & 0 \\ 0 & U \end{bmatrix} = \begin{bmatrix} \bar{K} & 0 \\ 0 & \Omega_g \end{bmatrix}$$

$$[\hat{M}_k] = \begin{bmatrix} I & 0 \\ 0 & U^T \end{bmatrix} \begin{bmatrix} \bar{M} & \bar{M}_c \\ \bar{M}_c^T & M_g \end{bmatrix} \begin{bmatrix} I & 0 \\ 0 & U \end{bmatrix} = \begin{bmatrix} \bar{M} & M_c \\ M_c & I \end{bmatrix} \quad (19)$$

Finally, the mass normalized eigenvectors Ψ_k in Eq. (9) can be obtained as the eigensolution of the test models of Eq. (19).

SEREP-CB Transformation and Its Application to the System Identification

The $n \times n$ Craig-Bampton finite element models of Eqs. (7) and (8) have by far more DOF than the $k \times k$ test models of Eq. (19). Therefore, the Craig-Bampton finite element models, which are obtained from the initial finite element models, should be reduced to match with the DOF of test models for the generation of the present TAM. As the reduction method of this paper, the SEREP¹¹ method is used somewhat differently after eigenvectors chosen at generalized coordinates are included in the generalized inverse of the SEREP method. When the k eigenvectors are retained from the eigensolutions of the Craig-Bampton finite element models, the $n \times k$ modal matrix is given as

$$[\Phi] = [\phi_1 \quad \phi_2 \quad \cdots \quad \phi_k] = \begin{bmatrix} \Phi_m \\ \Phi_\xi \end{bmatrix} \quad (20)$$

where $i = 1, \dots, k$ represent the individual eigenvectors and Φ_m and Φ_ξ denote the $m \times k$ and $(n - m) \times k$ modal submatrices corresponding to the measured and generalized coordinate DOF of Φ , respectively. The modal matrix Φ_ξ is partitioned into the $\Phi_{\xi a}$ and $\Phi_{\xi b}$, and then the Φ_m and $\Phi_{\xi a}$ are merged to the Φ_k as follows:

$$[\Phi] = \begin{bmatrix} \Phi_m \\ \Phi_{\xi a} \\ \cdots \\ \Phi_{\xi b} \end{bmatrix} = \begin{bmatrix} \Phi_k \\ \Phi_{\xi b} \end{bmatrix} \quad (21)$$

where $\Phi_{\xi a}$, $\Phi_{\xi b}$, and Φ_k are $(k - m) \times k$, $(n - k) \times k$, $k \times k$ modal submatrices, respectively. Until now, the modal submatrix Φ_m , which is the eigenvector chosen only at the measured DOF, has been applied to the generalized inverse of the SEREP method. But the modal matrix Φ_k , which includes the submatrix corresponding to the generalized coordinates, is applied to the generalized inverse of the SEREP transformation matrix as follows:

$$[T_{\text{SEREP}}] = \begin{bmatrix} \Phi_k \\ \Phi_{\xi b} \end{bmatrix} [\Phi_k]^{-1} \quad (22)$$

Therefore, using the Craig-Bampton transformation matrix of Eq. (6) and the SEREP transformation matrix of Eq. (22), the present TAM can be generated from the initial finite element model of Eq. (2) as follows:

$$[\hat{M}_k] = [T_{\text{SEREP}}]^T [T_{\text{CB}}]^T [M_n] [T_{\text{CB}}] [T_{\text{SEREP}}]$$

$$[\hat{K}_k] = [T_{\text{SEREP}}]^T [T_{\text{CB}}]^T [K_n] [T_{\text{CB}}] [T_{\text{SEREP}}] \quad (23)$$

Here, the SEREP-CB transformation matrix used for the present TAM is defined as

$$[T_{\text{mix}}] = [T_{\text{CB}}] [T_{\text{SEREP}}] \quad (24)$$

The present TAM of Eq. (23) are used for the direct correction of the stiffness matrix of the initial finite element models. For such corrections, submatrices with scaling factors representing a perturbation from the initially assumed stiffness are used.⁴ Submatrices are made by grouping the elements of the same stiffness characteristics, which can be used for modeling the unknown stiffness of connected parts. The stiffness matrix of the initial finite element model of Eq. (1) is expanded into a linear sum of submatrices, such as

$$[K_n] = \left\{ [K_b] + \sum_{j=1}^p [K_j] \right\} + \sum_{j=1}^p s_j [K_j] = [K_a] + \sum_{j=1}^p s_j [K_j] \quad (25)$$

where p is the total number of submatrices. Matrices in Eq. (25) are known so that scaling factors s_j should be determined to update $[K_a]$. First, the present transformation matrix of Eq. (24) is applied to the initial finite element models of Eq. (1) having submatrices of Eq. (25). Then, the system identification equation for unknown scaling factors s_j can be formulated as the following linear equation:

$$\sum_{j=1}^p s_j [\tilde{K}_j] [\Psi_k] = [\tilde{M}_k] [\Psi_k] [\Omega_k] - [\tilde{K}_a] [\Psi_k] \quad (26)$$

where

$$[\tilde{K}_j] = [T_{\text{mix}}]^T [K_j] [T_{\text{mix}}], \quad [\tilde{K}_a] = [T_{\text{mix}}]^T [K_a] [T_{\text{mix}}]$$

$$[\tilde{M}_k] = [T_{\text{mix}}]^T [M_n] [T_{\text{mix}}] \quad (27)$$

and the diagonal matrix $[\Omega_k]$ is composed of k -measured eigenvalues of the modal test. The modal matrix $[\Psi_k]$ is obtained from the eigensolutions of the test model of Eq. (19) and expressed in Eq. (9).

Column vectors of Eq. (26) can be defined as

$$\{L_{ji}\} = [\tilde{K}_j] \{\psi_i\}, \quad j = 1, 2, \dots, p \quad \text{and} \quad i = 1, 2, \dots, k \quad (28)$$

$$\{R_i\} = [\tilde{M}_k] \{\psi_i\} \Omega_i - [\tilde{K}_a] \{\psi_i\}$$

$$j = 1, 2, \dots, p \quad \text{and} \quad i = 1, 2, \dots, k \quad (29)$$

The system identification equation (26) is obtained as

$$[L] \{s\} = \{r\} \quad (30)$$

where

$$[L] = \begin{bmatrix} \{L_{11}\} & \{L_{21}\} & \cdots & \{L_{p1}\} \\ \{L_{12}\} & \{L_{22}\} & \cdots & \{L_{p2}\} \\ \vdots & \vdots & \ddots & \vdots \\ \{L_{1k}\} & \{L_{2k}\} & \cdots & \{L_{pk}\} \end{bmatrix} \quad (31)$$

$$\{s\} = \{s_1 \quad s_2 \quad \cdots \quad s_p\}^T \quad (32)$$

$$\{r\} = \{\{R_1\}^T \quad \{R_2\}^T \quad \cdots \quad \{R_k\}^T\}^T \quad (33)$$

Finally, unknown scaling factors s_j of Eq. (30) are solved by using a least-square method because the number of unknown scaling factors are generally much smaller than column vector size. Therefore, the parametric correction of the initial finite element models can be performed by substituting scaling factors into Eq. (25). In the system identification equation of Eq. (30), the mass matrix is assumed to be modeled accurately. If the mass matrix is also desired to correct, the mass submatrices⁵ with scaling factors are simply added to Eq. (26).

If the Guyan TAM is used for the correction as in Ref. 4, the system identification equation (26) becomes

$$\sum_{j=1}^p s_j [\bar{K}_j] [\Psi_m] = [\bar{M}] [\Psi_m] [\Omega_m] - [\bar{K}_a] [\Psi_m] \quad (34)$$

where $[\Psi_m]$ and $[\Omega_m]$ are measured modes and eigenvalues, respectively, and $[\bar{K}]$ and $[\bar{M}]$ are the Guyan-reduced matrices of stiffness and mass, respectively.

If the correction of the initial stiffness model is not within 5% error, the iteration procedures for Eq. (26) are continued. Here, the error percent is defined as

$$\text{error percent} = (\Omega_i - \Omega_c) / \Omega_i \times 100 \quad (35)$$

where Ω_i and Ω_c are the measured and corrected eigenvalue, respectively. The corrected stiffness in the i th iteration is defined as follows:

$$K_j^{(i)} = [1 + s_j^{(1)}][1 + s_j^{(2)}] \cdots [1 + s_j^{(i)}] K_j^{(0)} \quad (36)$$

where the subscript j , the superscript (i) , and $K_j^{(0)}$ denote the number of the j th submatrix, the iteration number, and the initially assumed stiffness, respectively.

Numerical Simulation Results

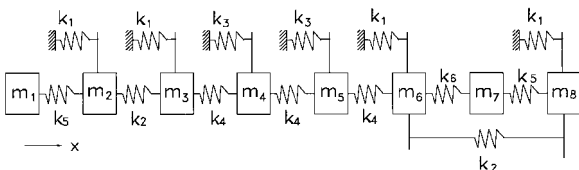
Application to Kabe's Model

To illustrate the stiffness correction using a present TAM, a numerical example used by Kabe¹ is chosen. This model includes 8 masses and 14 springs with connectivity as shown in Fig. 1. In this example the mass matrix is assumed exact, and the stiffness matrix is to be corrected using measured modal test data. The masses are constrained to translate in the x direction only. The spring constants, which were used to compose the initial model and exact model, are presented in Table 1. Initial spring constants of the initial model are improved by using modal test data simulated from the exact model. The dynamic characteristics of the initial and exact model are presented in Table 2. The nonzero upper triangular stiffness coefficients of the initial and exact model are shown in Table 3 according to the consistency conditions.

Prior to the correction using a present TAM, one should review how sensitive to the measurement locations the reduction accuracy of Guyan TAM is. Also the stiffness correctness related with the reduction accuracy is additionally reviewed. For such review x_2, x_4, x_6, x_7 , and x_8 are selected in Fig. 1 for case I and x_2, x_5, x_6, x_7 , and x_8 are selected for case II as the measurements of a modal test. The eigenvalues calculated from the Guyan TAM of the initial model are presented in Table 4 for cases I and II. Although only one point x_5 of case II is differently chosen from the point x_4

Table 1 Spring constants in the initial model and exact model

Spring ID	Initial spring constant	Exact spring constant
k_1	40	50
k_2	50	40
k_3	40	60
k_4	20	20
k_5	45	30
k_6	15	10



$$m_1=m_3=m_5=0.05, \quad m_2=m_4=m_6=m_8=1.0, \quad m_7=0.5$$

Fig. 1 Eight-DOF Kabe model.

Table 2 Comparison between the initial and exact models

Mode number	Eigenvalue, (rad/s) ²	
	Exact model	Initial model
1	37.6	34.0 (9.6) ^a
2	68.7	57.3 (16.6)
3	93.9	76.9 (18.1)
4	114.0	140.6 (−23.3)
5	164.6	200.2 (−21.6)
6	633.7	947.5 (−49.5)
7	2008.3	1610.6 (19.8)
8	2219.2	2228.0 (−0.4)

^aError percent of Eq. (35).

of case I, the Guyan TAM of case II cannot preserve the dynamic characteristics of the initial model compared with case I. These results demonstrate that Guyan TAM may become a very inaccurately reduced model according to the measurement locations. When the Guyan TAM for cases I and II is used in Eq. (34), the corrected stiffness and eigenvalues are presented in Tables 3 and 4, respectively. For solving Eq. (34) with a least-square method, two mode shapes calculated from the exact model are used as the measured mode shapes in Eq. (34). These corrected stiffness and eigenvalues are obtained without any iterative calculation of Eq. (36). As shown in Table 4, the correctness of the initial model is related with the accuracy of reduced models.⁴ The Guyan TAM of case I results in a good correction of the initial model, but the Guyan TAM of case II does not improve the initial model in the further iterative calculations of Eq. (36).

To demonstrate the accuracy of the present TAM in comparison with the Guyan TAM, four points, which are one point smaller than points chosen in cases I or II, are selected as the measurement locations. As the measurement locations x_1, x_2, x_4 , and x_7 are chosen in Fig. 1 for case III, and x_3, x_5, x_6 , and x_8 are chosen for case IV. For the generation of the test model using the minimal-order resultant mass and stiffness matrices, the six eigenvectors and eigenvalues are extracted from modal test results for cases III and IV. Here, the modal test results are simulated from the exact model. The matrix size of the test model is 6×6 , whose DOF consists of four measurement DOF and two generalized coordinate DOF. The eigenvalues calculated from this test model for cases III and IV are exactly the same as eigenvalues extracted directly from the exact model, so that these eigenvalue results are not included in Table 5. The test model obtained from the minimal-order resultant mass and stiffness matrices can retain all measured modal parameters. In the meanwhile, to get the present TAM the SEREP-CB transformation is applied to the initial model. The eigenvalues calculated directly from the present TAM of the initial model are presented in Table 5, where the present TAM preserves the dynamics of the initial model up to the sixth mode, regardless of the measurement locations chosen in cases III or IV. On the contrary to the present TAM, the Guyan TAM cannot preserve the dynamics of the initial model in any cases III or IV. The corrected stiffness and eigenvalues obtained by using a present TAM are presented in Tables 3 and 5, respectively. Here, six mode shapes and eigenvalues obtained from the test model are used as the measured modal data for the generation of column vectors $\{L_{ji}\}$ and $\{R_i\}$ of Eq. (30). To correct the initial model within the 5% error, just a few iterations are performed. Even though cases III and IV have smaller measurement points than cases I and II, the present TAM for cases III and IV can be successfully applied to the model updating of the initial model regardless of measurement locations.

Application to a Cantilever Beam

As another illustration of the stiffness correction using a present TAM, a cantilever is modeled with 20 finite element beams of equal length. The exact model is a continuous cantilever beam, whereas the initial model is composed of two beams of half-length of the exact model, as shown in Fig. 2. The joint stiffness of the initial model is modeled with two springs, whose properties are initially assumed as $k_1 = 15$ kgf/mm and $k_2 = 20$ kgf-mm/rad. And no clearance is assumed in the joint part. The assumed springs have the translational and rotational DOF as the finite element beam does.

Table 3 Nonzero upper triangular stiffness matrix coefficients of the initial, exact, and corrected models

Coefficient location in stiffness matrix	Consistency condition	Exact stiffness coefficient	Initial stiffness coefficient	Corrected stiffness coefficient			
				Guyan TAM		Present TAM	
				Case I	Case II	Case III	Case IV
1,1	k_5	30.0	45.0	28.6	29.4	32.6	30.0
1,2	$-k_5$	-30.0	-45.0	-28.6	-29.4	-32.6	-30.0
2,2	$k_1 + k_2 + k_5$	120.0	135.0	114.9	106.9	119.5	120.8
2,3	$-k_2$	-40.0	-50.0	-36.4	-23.8	-37.4	-41.7
3,3	$k_1 + k_2 + k_4$	110.0	110.0	106.6	86.0	102.8	99.3
3,4	$-k_4$	-20.0	-20.0	-20.2	-8.5	-15.9	-8.5
4,4	$k_3 + 2k_4$	100.0	80.0	99.5	43.8	97.9	94.9
4,5	$-k_4$	-20.0	-20.0	-20.2	-8.5	-15.9	-8.5
5,5	$k_3 + 2k_4$	100.0	80.0	99.5	43.8	97.9	94.9
5,6	$-k_4$	-20.0	-20.0	-20.2	-8.5	-15.9	-8.5
6,6	$k_1 + k_2 + k_4 + k_6$	120.0	125.0	117.6	96.4	113.0	111.3
6,7	$-k_6$	-10.0	-15.0	-11.0	-10.4	-10.2	-12.0
6,8	$-k_2$	-40.0	-50.0	-36.5	-23.8	-37.4	-41.7
7,7	$k_5 + k_6$	40.0	60.0	39.6	39.8	42.8	42.1
7,8	$-k_5$	-30.0	-45.0	-28.6	-29.4	-32.6	-30.0
8,8	$k_1 + k_2 + k_5$	120.0	135.0	114.9	106.9	119.5	120.8

Table 4 Corrected eigenvalues (rad/s)², using the Guyan TAM for the eight DOF Kabe model

Mode number	Exact model	Initial model		Corrected model ^a		
		Before reduction	After reduction			
			Case I	Case II	Case I	Case II
1	37.6	34.0	34.0	34.0	37.5 (0.1) ^b	37.4 (0.5)
2	68.7	57.3	57.5	61.2	67.5 (1.9)	41.1 (40.2)
3	93.9	76.9	77.0	139.4	92.8 (1.1)	67.1 (28.5)
4	114.0	140.6	140.6	199.9	114.1 (-0.1)	103.6 (9.2)
5	164.6	200.2	200.2	643.5	156.3 (5.1)	140.0 (15.0)
6	633.7	947.5	—	—	604.4 (4.6)	620.7 (2.1)
7	2008.3	1610.6	—	—	1999.5 (0.4)	879.2 (56.2)
8	2219.2	2228.0	—	—	2148.6 (3.2)	1728.8 (22.1)

^aRef. 4. ^bError percent of Eq. (35).

Table 5 Corrected eigenvalues (rad/s)², using a present TAM for the eight-DOF Kabe model

Mode number	Exact model	Before reduction	Initial model		Present TAM		Corrected model	
			Guyan TAM		Case III	Case IV	Case III	Case IV
			Case III	Case IV				
1	37.6	34.0	43.6	36.9	34.0	34.0	37.3 (0.3) ^a	36.1 (1.9)
2	68.7	57.3	57.4	158.9	57.3	57.3	67.6 (0.8)	68.3 (0.3)
3	93.9	76.9	77.0	172.2	76.9	76.9	93.8 (0.0)	93.9 (0.0)
4	114.0	140.6	947.9	768.9	140.6	140.6	114.9 (-0.4)	114.9 (-0.4)
5	164.6	200.2	—	—	200.2	200.2	163.3 (0.4)	164.4 (0.1)
6	633.7	947.5	—	—	947.5	947.5	687.3 (-4.1)	633.7 (0.0)
7	2008.3	1610.6	—	—	—	—	1963.9 (1.1)	1900.1 (2.7)
8	2219.2	2228.0	—	—	—	—	2073.5 (3.3)	2004.4 (5.0)

^aError percent of Eq. (35).

Therefore, the problem is to correct the assumed stiffness of the joint part to simulate the continuous beam of the exact model. The finite element beam of a circular cross section is modeled with the steel property as $E = 21,092.4 \text{ kgf/mm}^2$, $\rho = 7.8 \times 10^{-6} \text{ kg/mm}^3$, length = 20 mm, and diameter = 3 mm. The mass and stiffness matrices for the initial model are then of size 42×42 . Here the mass matrix is assumed to be modeled accurately. The initial model has two assumed springs so that the number of submatrices used for updating the stiffness is two.

As the measurement points of a modal test, the eight and four transverse DOF are chosen for cases V and VI, respectively, as shown in Fig. 2. Here, the modal test results are simulated from the continuous beam of the exact model. In case V, 11 eigenvectors and eigenvalues are extracted from the modal test results for the generation of the test model using the minimal-order resultant mass and stiffness matrices. So, the matrix size of the test model, which includes three generalized coordinates, is 11×11 in case V. In case

VI, seven eigenvectors and eigenvalues are chosen from the modal test results so that the matrix size of the test model is 7×7 , where three generalized coordinates are included. Meanwhile, the 42×42 initial model is reduced according to the DOF of the test model of cases V and VI. The eigenvalue results calculated directly from the present TAM of cases V and VI are presented in Table 6, where the present TAM is shown to preserve the dynamics of the initial model regardless of the number of measurement points. On the other hand, the Guyan TAM cannot preserve the dynamics of the initial model in any case.

For the correction of the initial model using the present TAM of cases V and VI, measured modal data are obtained from the test model of each case as before. When the 11×11 TAM of case V is used for the correction, 7 modes and 11 modes are respectively used as the measured modal data for the generation of column vectors $\{L_{ji}\}$ and $\{R_i\}$ of Eq. (30). In case VI, whose TAM size is 7×7 , five modes and seven modes are respectively used as the measured modal

Table 6 Corrected natural frequencies (Hz), using the present TAM for a cantilever beam

Initial model								
Mode number	Exact model	Before reduction	Guyan TAM		Present TAM		Corrected model	
			Case V	Case VI	Case V	Case VI	Case V	Case VI
1	13.5	5.6	5.6	5.6	5.6	5.6	13.5 (0.0) ^a	13.5 (0.0)
2	84.7	40.3	40.3	40.4	40.3	40.3	82.0 (3.2)	80.9 (4.5)
3	237.2	235.9	242.3	281.1	235.9	235.9	237.0 (0.1)	237.0 (0.1)
4	464.8	344.4	361.2	468.5	344.4	344.4	450.7 (3.0)	445.4 (4.2)
5	768.1	754.4	804.9	—	754.4	754.4	765.8 (0.3)	765.8 (0.3)
6	1147.2	951.2	1109.4	—	951.2	951.2	1114.0 (2.9)	1102.6 (3.9)
7	1602.0	1573.4	2423.3	—	1573.4	1573.4	1591.6 (0.6)	1591.7 (0.6)
8	2132.7	1861.1	4906.6	—	1861.1	—	2073.9 (2.8)	2055.0 (3.6)
9	2739.8	2528.3	—	—	2528.3	—	2708.4 (1.1)	2708.6 (1.1)
10	3423.7	3075.4	—	—	3075.4	—	3333.4 (2.6)	3306.2 (3.4)
11	4185.4	3665.7	—	—	3665.7	—	4108.6 (1.8)	4109.2 (1.8)

^aError percent of Eq. (35).

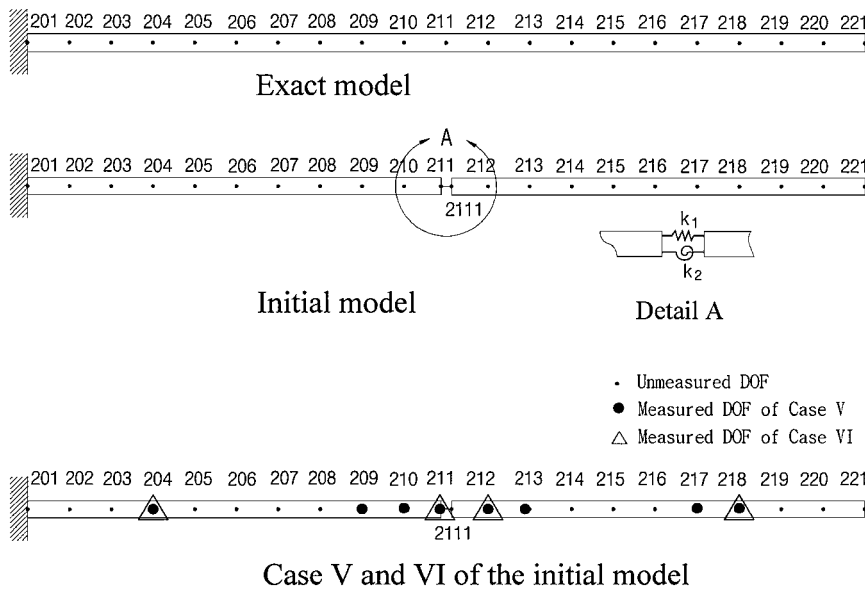


Fig. 2 Finite element model of a cantilever beam.

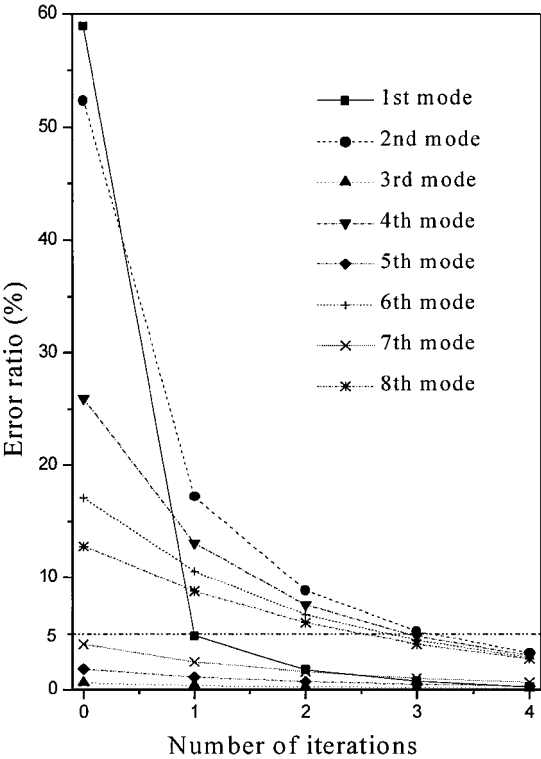


Fig. 3 Error ratio of eigenvalues calculated from the corrected model in case V with 11 modes used in Eq. (30).

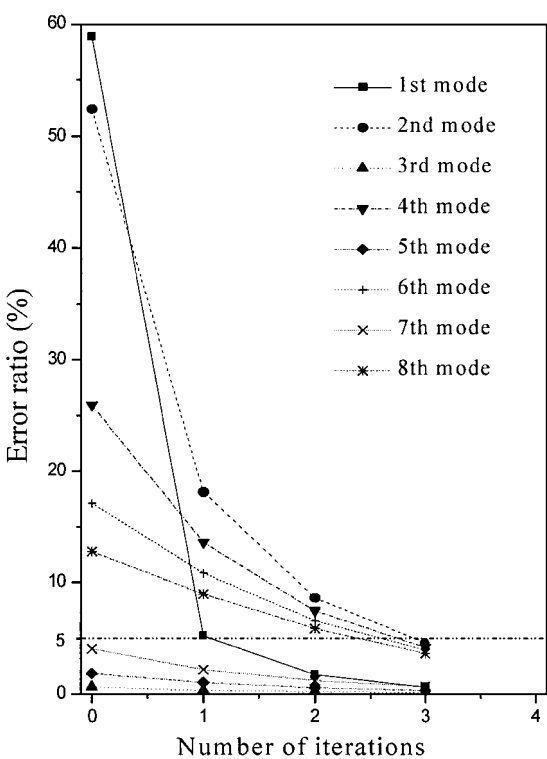
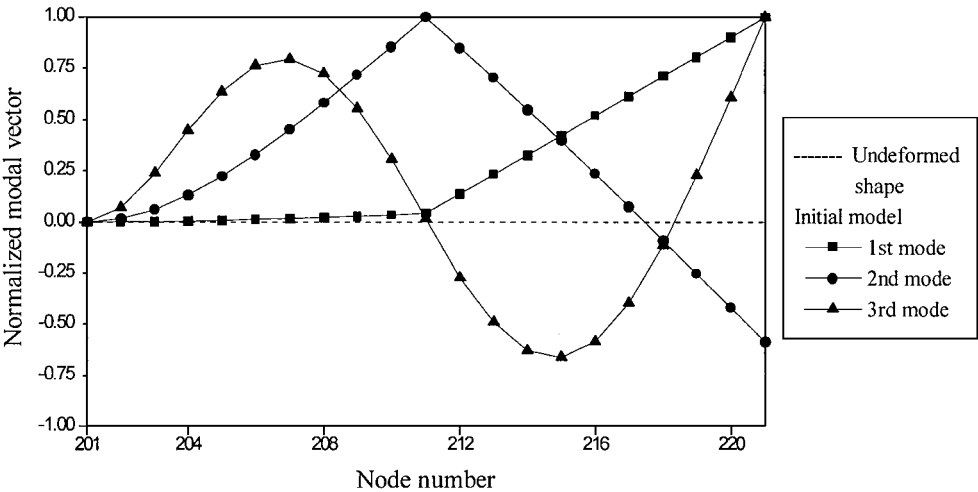


Fig. 4 Error ratio of eigenvalues calculated from the corrected model in case VI with seven modes used in Eq. (30).

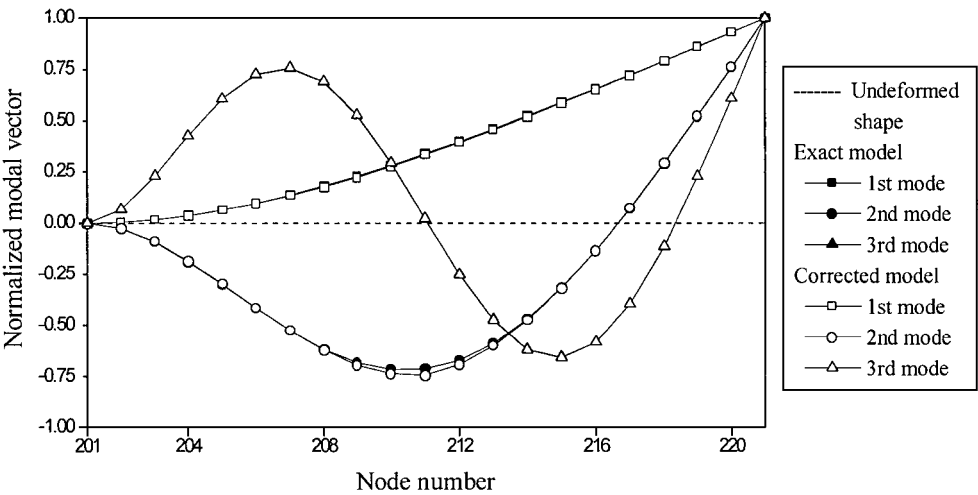
Table 7 Corrected stiffness of assumed spring

Stiffness type	Exact value	Initial value	Corrected value			
			Case V		Case VI	
			7 ^a , 27 ^b	11 ^a , 4 ^b	5 ^a , 12 ^b	7 ^a , 3 ^b
k_1 , kgf/mm	241.0	15.0	35.8	85.7	35.6	86.2
k_2 , kgf-mm/rad	32,488.6	20.0	11,262.2	6,149.3	7,406.0	4,284.2

^aNumber of modes used in Eq. (30). ^bNumber of iteration within the error ratio of 5%.



a) Mode shapes of the initial model



b) Mode shapes of the corrected and exact model

Fig. 5 Mode shapes of the cantilever beam.

data for the generation of column vectors of Eq. (30). According to the numbers of modes used in Eq. (30) in each case, the numbers of iteration within the error of 5% and the corrected stiffness values are presented in Table 7. As shown in Table 7, the good convergence rate is obtained when the number of modes used in Eq. (30) is equal to the number of DOF of TAM. Table 7 also shows that corrected stiffness values of assumed springs are not uniquely determined in each case because of the characteristics of the least-square method. However, these stiffness values compose the solution group for the assumed springs. When 11 modes in case V are used in Eq. (30) and seven modes in case VI are used in Eq. (30), the iterative procedures of corrected eigenvalues are presented in terms of error ratio in Figs. 3 and 4, respectively. For the preceding cases the corrected eigenvalues are also listed in Table 6, and the mode shapes obtained from these corrected models are presented in Fig. 5, where the mode shapes of the corrected and exact model are in a good agreement.

Conclusion

An improved approach is presented to update the initial finite element models with the reduced models dynamically equivalent to the initial models. The previously reported TAM used for the correction of the initial model, particularly Guyan TAM, is composed of only measured DOF in the modal test. The classical Guyan TAM cannot retain the dynamics of the initial model according to the measurement points. Therefore, the generalized coordinates are additionally included in the present reduction method to take into account the inertia force effect at unmeasured DOF. The present TAM is formulated by applying consecutively the Craig–Bampton transformation and the SEREP transformation to the initial finite element model. Modal matrices used for the SEREP method are obtained from the eigensolutions of the Craig–Bampton finite element models. Particularly, the modal matrix used in the inverse matrix of the SEREP method includes eigenvectors of the generalized coordinate DOF other than the measured DOF. The generalized coordinate DOF of

the present TAM are determined according to the test model. This test model is obtained from the minimal-order resultant mass and stiffness matrices when the identified modes of a modal test are more than accelerometers. Therefore, the present TAM can preserve the dynamics of the initial finite element model regardless of measurement points and can be used for a direct analysis/experiment correlation with modal parameters obtained from the test model.

To solve the problem, the stiffness matrices of the initial model are expanded into a linear sum of submatrices having scaling factors. The scaling factors of submatrices are solved by the least-square method. Simulation results for Kabe's model and cantilever beam demonstrate that the present TAM can preserve the dynamics of the initial model regardless of measurement points, so that this TAM can be successfully applied to correct the initial model with the modal parameters obtained from the test model.

References

- ¹Kabe, A. M., "Stiffness Matrix Adjustment Using Mode Data," *AIAA Journal*, Vol. 23, No. 9, 1985, pp. 1431–1436.
- ²Guyan, R. J., "Reduction of Stiffness and Mass Matrices," *AIAA Journal*, Vol. 3, No. 2, 1965, p. 380.
- ³O'Callahan, J. C., "A Procedure for an Improved Reduced System (IRS) Model," *Proceedings of the 7th International Modal Analysis Conference*, Union College, Schenectady, NY, 1989, pp. 17–21.
- ⁴Lim, T. W., "Submatrix Approach to Stiffness Matrix Correlation Using Modal Test Data," *AIAA Journal*, Vol. 28, No. 6, 1990, pp. 1123–1130.
- ⁵Lim, T. W., "Analytical Model Improvement Using Measured Modes and Submatrices," *AIAA Journal*, Vol. 29, No. 6, 1991, pp. 1015–1018.
- ⁶Kammer, D. C., and Flanigan, C. C., "Development of Test-Analysis Models for Large Space Structures Using Substructure Representations," *Journal of Spacecraft and Rockets*, Vol. 28, No. 2, 1991, pp. 244–250.
- ⁷Razzaque, A., "The Irons-Guyan Reduction Method with Iterations," *Proceedings of the 10th International Modal Analysis Conference*, Union College, Schenectady, NY, 1992, pp. 137–145.
- ⁸Denoyer, K. K., and Peterson, L. D., "Method for Structural Model Update Using Dynamically Measured Static Flexibility Matrices," *AIAA Journal*, Vol. 35, No. 2, 1997, pp. 362–368.
- ⁹Alvin, K. F., Peterson, L. D., and Park, K. C., "Method for Determining Minimum Order Mass and Stiffness Matrices from Modal Test Data," *AIAA Journal*, Vol. 33, No. 1, 1995, pp. 128–135.
- ¹⁰Craig, R. R., and Bampton, M. C., "Coupling of Substructures for Dynamic Analysis," *AIAA Journal*, Vol. 6, No. 7, 1968, pp. 1313–1319.
- ¹¹O'Callahan, J. C., Avitabile, P., and Riemer, R., "System Equivalent Reduction Expansion Process (SEREP)," *Proceedings of the 7th International Modal Analysis Conference*, Union College, Schenectady, NY, 1989, pp. 29–37.

A. Berman
Associate Editor